What Sets the Surface Eddy Mass Flux in the Southern Ocean?

S. S. DRIJFHOUT

Royal Netherlands Meteorological Institute (KNMI), De Bilt, Netherlands

ABSTRACT

The Ocean Circulation and Climate Advanced Modelling (OCCAM) global, eddy-permitting ocean general circulation model has been used to investigate the surface eddy mass flux in the Southern Ocean. The isopycnal eddy mass flux in the surface layer is almost uniformly poleward and scales well with the local Ekman transport. This seems at odds with other models and observations suggesting topographic localization of the eddy fluxes with locally, large rotational components. Integrated over the thermocline depth the eddy fluxes do show such topographic localization. The surface eddy mass flux is mainly a consequence of the intermittent deepening of the mixed layer with the seasonal cycle, which redistributes the Ekman transport over the stack of layers that eventually become ventilated. Baroclinic instability gives rise to much smaller eddy-induced transports. Independent of the framework in which the residual mean flow is analyzed (isopycnal or geometric), the eddy-induced transport that opposes the wind-driven Ekman flow only partially compensates the Deacon cell. The associated overturning cell is about 5 Sv (where $1 \text{ Sv} \equiv 10^6 \text{ m}^3 \text{ s}^{-1}$), responsible for a cancellation of the Deacon cell of 30%. In geometric coordinates, a strong signature (14 Sv) of the Deacon cell remains for the residual mean flow. Only after transformation to density coordinates is a further reduction with 10 Sv obtained. Zonal tilting of isopycnals makes along-isopycnal recirculations appear as vertical overturning cells in geometric coordinates. These cells disappear in the isopycnal framework without any eddy-induced transport being involved.

1. Introduction

In many places in the World Ocean eddy fluxes seem to counteract the Ekman transport. Consequently, their signature in the surface layer should be strong—of the same order of magnitude as the Ekman flux itself. As a result, in the Southern Ocean the residual mean flow near the surface (being the sum of the Eulerian mean flow and an eddy-induced flow) differs strongly from the Eulerian mean circulation. An observational estimate of the eddy fluxes, however, is difficult to get. There are few measurements in the Southern Ocean, localized in space and time, which allow the eddy fluxes to be calculated (Bryden and Heath 1985; Johnson and Bryden 1989; Phillips and Rintoul 2000; Gille 2003). The eddy fluxes tend to be downgradient, but the measurements are too short and too sparse to allow a quantitative estimate for the whole Southern Ocean.

Most of the eddy variability in the Southern Ocean can be associated with the baroclinic instability of the Antarctic Circumpolar Current (ACC). It is tentative to estimate eddy fluxes from a closure that relates them to the large-scale gradient of the relevant quantity (most often buoyancy). Such an eddy diffusivity model is basically an elaboration of the Gent and McWilliams (1990) parameterization, which relates the eddy fluxes to the local isopycnal slope. In modeling studies, the strength of the diffusivity is often determined by scaling relations that express the diffusivity as a function of both internal and external parameters (Visbeck et al. 1997; Karsten et al. 2002). In observational studies some of these parameters are less easily estimated and most often the approach of Holloway (1986) is followed, which relates the diffusivity to sea surface height (SSH) variability estimated from satellite altimetry.

Satellite altimetry confirms the picture that most eddy variability in the extratropical World Ocean may be associated with baroclinic instability; SSH variability is concentrated in boundary currents and the ACC (Stammer 1997). A closer inspection reveals that eddy variability in the ACC is enhanced downstream of the major topographic features in the Southern Ocean. Many modeling studies also show localization of eddy

Corresponding author address: S. S. Drijfhout, Royal Netherlands Meteorological Institute (KNMI), P.O. Box 201, 3730 AE De Bilt, Netherlands.
E-mail: drijfhou@knmi.nl
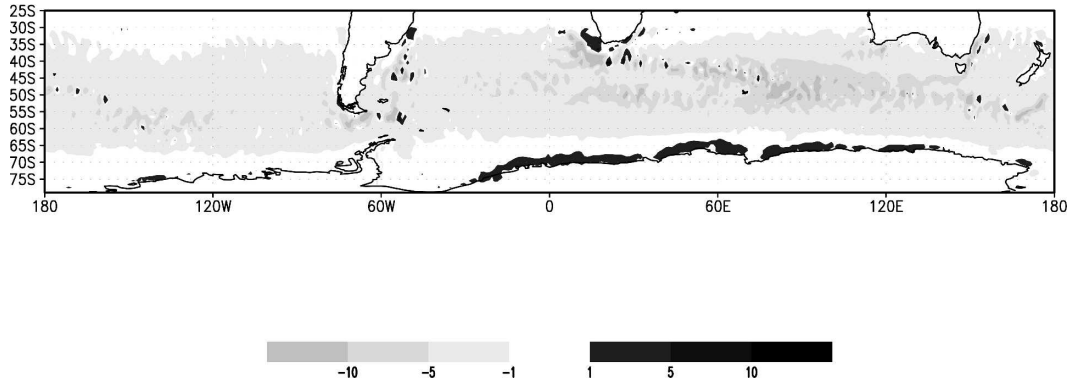
FIG. 1. Upper-layer eddy-induced northward velocity (cm s^{-1}) for the Southern Ocean poleward of 25°S. Values are averaged for grid boxes of 1° by 1°. Positive values are northward. The eddy-induced velocity is calculated in an isopycnal framework.

fluxes downstream of topography (Gille 1997; Best et al. 1999; Hallberg and Gnanadesikan 2001; MacCready and Rhines 2001). This localization results from the topography destabilizing the flow. The aforementioned models, however, either do not explicitly address the surface layer, or they are rather idealized, especially in their treatment of the upper, forced layer. Nevertheless, the results suggest that part of the Ekman flux is returned by the eddies in rather concentrated bands which necessitates a zonal redistribution of the meridional mass fluxes. Also, the eddy fluxes should feature large rotational components. Although topographic localization would result in violations of a local, eddy flux–isopycnal slope relation, in a zonal, or along-streamline integration, it would corroborate the assumption that the eddy flux is determined by baroclinic instability and potential energy release.

In an attempt to explain the large effect of eddy fluxes on the pathways that water masses follow in a numerical model, even in regions where the eddy fluxes associated with baroclinic instability should be small, Drijfhout et al. (2003) argued that compensation of the Ekman flow by eddy fluxes occurs locally. They calculated the ratio of the surface-layer, eddy mass flux to the Ekman flux and found that it was almost uniformly negative, with values in the Southern Ocean around −0.7. This result seems at odds with the idea of topographic localization that would result from baroclinic instability. Indeed, if the upper-layer, meridional eddy-induced velocity is plotted (Fig. 1), one sees that it is almost uniformly negative; and although there are some signs of a local enhancement, there is no evidence of a systematic and significant enhancement downstream of the topographic features that deflect the ACC. Nor is there any sign of a large rotational component of the eddy-induced mass flux, which would in-

evitable lead to regions with northward eddy-induced velocities.

The main question this paper addresses is whether the same baroclinic instability process that in other studies seems to determine the eddy-induced mass flux is active in the Ocean Circulation and Climate Advanced Modelling (OCCAM) model (Webb et al. 1997); and if so, why topographic localization is absent in the surface-layer, eddy-induced mass flux in OCCAM. Furthermore, the question is what other processes possibly determine the surface-layer, eddy-induced mass flux. This paper is organized as follows: it begins with a discussion of definitions of eddy-induced flow in geometrical and isopycnic coordinates. In section 3, it is discussed how the surface-layer, eddy-induced mass flux is calculated in OCCAM, and what the characteristics are of the time variability of the surface-layer meridional mass transport. In section 4, this time variability is related to the relevant transient processes in OCCAM. Section 5 gives a discussion on the role of the eddy-induced transport in the cancellation of the Deacon cell. A discussion on possible model biases and current parameterizations is given in section 6.

2. Isopycnic versus residual mean flow

In isopycnic coordinates adiabatic mass transport is naturally aligned along isopycnals, and cross-isopycnal flow corresponds with diabatic forcing. Within the framework, mass is advected by the thickness-weighted mean isopycnal velocity (Andrews et al. 1987):

$$\frac{\overline{vh}}{\overline{h}} = \overline{v} + \frac{\overline{v'h'}}{\overline{h}}, \tag{1}$$

where the variables have been separated into (zonal and time) mean quantities, $\overline{x}$ and perturbations about

this mean, x'. The mean meridional mass transport $V = vh$ obeys the continuity equation:

$$\frac{\partial \overline{V}}{\partial y} + \frac{\partial \overline{W}_e}{\partial \sigma} = 0, \tag{2}$$

where W_e is the diapycnal mass flux. An isopycnal streamfunction Ψ_i can be defined, with $\overline{V} = -\partial \Psi_i/\partial \sigma$ and $\overline{W}_e = -\partial \Psi_i/\partial y$. For adiabatic flow, Ψ_i is aligned along zonally averaged (isopycnal) depth.

Andrews and McIntyre (1976) defined a transformed Eulerian mean, or residual circulation in geometric coordinates, which has many features in common with the zonal-mean isopycnic (isentropic) mass circulation. The relevant equation to consider is now the buoyancy equation, which, after zonal and time averaging reads

$$\overline{v}\frac{\partial \overline{b}}{\partial y} + \overline{w}\frac{\partial \overline{b}}{\partial z} = Q - \frac{\partial \overline{v'b'}}{\partial y} - \frac{\partial \overline{w'b'}}{\partial z}, \tag{3}$$

where b is the buoyancy and Q is the buoyancy forcing. From Eq. (3) it is immediately seen that the Eulerian mean circulation is not aligned along zonal mean contours of b for adiabatic flow ($Q = 0$), because of the eddy terms that appear as forcing terms at the rhs of Eq. (3). In case of adiabatic flow, the eddy fluxes must be purely advective to compensate advection by the mean flow. When Eq. (3) is rewritten in terms of a residual circulation, the flow appears to be directly forced by Q:

$$(\overline{v} + \overline{v}*)\frac{\partial \overline{b}}{\partial y} + (\overline{w} + \overline{w}*)\frac{\partial \overline{b}}{\partial z} = Q, \tag{4}$$

where

$$\overline{v}* = \frac{\partial \overline{v'b'}}{\partial y} \bigg/ \frac{\partial \overline{b}}{\partial y} \tag{5}$$

and

$$\overline{w}* = \frac{\partial \overline{w'b'}}{\partial z} \bigg/ \frac{\partial \overline{b}}{\partial z}. \tag{6}$$

Unlike $\overline{v}$ and $\overline{w}$, $\overline{v}*$ and $\overline{w}*$ are not divergence free. To overcome this, the eddy-induced transport has to be associated with a streamfunction $\Psi*$ with $\overline{v}* = -\partial \Psi*/\partial z$ and $\overline{w}* = -\partial \Psi*/\partial y$. Inspection of Eq. (3) suggests two alternative formulations for $\Psi*$ (with subscripts denoting differentiating), namely

$$\Psi* = -\frac{\overline{w'b'}}{\overline{b}_y} \quad \text{and} \tag{7}$$

$$\Psi* = \frac{\overline{v'b'}}{\overline{b}_z}. \tag{8}$$

Now the eddy-induced transport has been made divergence free, but it leaves a residual as compared with

Eqs. (5) and (6) (Eden et al. 2004, manuscript submitted to *J. Phys. Oceanogr.*). This residual tends to zero when the eddy-induced transport is along isopycnals, but it is likely to be large when the diabatic forcing is strong. The residual can be interpreted as as an extra eddy-forcing term in the buoyancy equation (Held and Schneider 1999; Marshall and Radko 2003), but is often neglected. With the definition of Eq. (8), the residual transport $\overline{v}_{res}$ is similar to its definition in the isopycnal framework given by Eq. (1), namely,

$$\overline{v}_{res} = \overline{v} - \frac{\partial}{\partial z}\left(\frac{\overline{v'b'}}{\overline{b}_z}\right). \tag{9}$$

McIntosh and McDougall (1996) show that

$$\frac{\overline{vh}}{\overline{h}} = \overline{v} - \frac{\partial}{\partial z}\left(\frac{\overline{v'b'}}{\overline{b}_z}\right) + O(\alpha^3), \tag{10}$$

where α symbolizes the perturbation amplitude. In general α can be assumed to be small, but near the surface this is not the case. When isopycnals outcrop the deviation of interface depth from its average value is $O(1)$, and so is α. Near the surface $\overline{b}_z$ may go to zero, and for this reason the definition for the eddy-induced transport of Eq. (7) is often preferred, although the connection with the isopycnal mass transport given by Eq. (1) is less clear. In either case the residual transport and isopycnal mass transport deviate significantly in the upper layers of the ocean.

In the present paper the eddy-induced transport will be discussed in the isopycnal framework, as this is the only way to guarantee that the inferred meridional overturning complies with the net isopycnal and diapycnal transport of the flow and, through the latter, with the net diabatic forcing.

3. Construction of the eddy-induced velocity

The annual mean velocity field, as well as the eddy-induced, or quasi-Stokes velocities, has been constructed from 219 archived 5-day averages from model years 9.0 to 12.0 of the OCCAM integration. The model has 36 levels in the vertical and a uniform horizontal resolution of 1/4° by 1/4°. The wind forcing was defined from 6-hourly European Centre for Medium-Range Weather Forecasts (ECMWF) winds. Years 9.0–12.0 of the model use wind stresses from 1993 to 1995 inclusively. Buoyancy fluxes were derived from relaxing the sea surface temperature and salinity to the Levitus 1994 climatology. The upper layer has a thickness of 20 m.

The eddy-induced velocity is defined as the difference between the thickness-weighted mean isopycnal velocity and Eulerian mean velocity [Eq. (1)]. The thickness-weighted mean isopycnal velocity is derived

from the isopycnal mass transport, which is calculated by transforming the 5-day averaged velocities from z to density (σ) coordinate. Last, the thickness-weighted mean isopycnal velocity and eddy-induced velocity are transformed back to z coordinates. The Eulerian mean transport is defined as

$$\overline{\mathbf{U}}(z) = \overline{\mathbf{u}}(z)\Delta z, \qquad (11)$$

where the bar denotes the time average, z is the vertical coordinate, Δz is the thickness of the grid box, and $\mathbf{u}(z)$ is the three-dimensional velocity. The Eulerian mean transport does not include contributions from seasonal variations and higher frequency eddies.

The residual mean isopycnal transport $\overline{\mathbf{U}}_R(z)$ and residual mean isopycnal velocity $\overline{\mathbf{u}}_R(z)$ are defined as

$$\overline{\mathbf{U_R}}(z) = \int_{\sigma_1}^{\sigma_2} \overline{\mathbf{U}}(\sigma)\, d\sigma/(\Delta\sigma) = \mathbf{u_R}(z)\Delta z, \qquad (12)$$

where σ_1 and σ_2 are defined as the densities levels whose annually averaged depth marks the vertical boundaries of the grid box at hand (McDougall 1998). To stress the difference between the residual mean flow determined in isopycnic coordinates, but transformed to geometric coordinates, and the residual mean flow determined in geometric coordinates [being the lhs and rhs, respectively, of Eq. (10)], I denote the former as the residual mean isopycnal (RMI) flow. The total mean thickness transport in a density layer is defined by

$$\overline{\mathbf{U}}(\sigma) = \overline{\mathbf{u}(\sigma)h(\sigma)}, \qquad (13)$$

where $h(\sigma)$ is the isopycnal layer thickness defined by the density interval $\Delta\sigma$ that is used to discretize the σ coordinate. For the calculation of the RMI transport a discretization of $\Delta\sigma = 0.01$ kg m^{-3} has been used. The eddy-induced velocity is simply given by

$$\mathbf{u}^*(z) = \overline{\mathbf{u_R}}(z) - \overline{\mathbf{u}}(z). \qquad (14)$$

The RMI velocity, Eulerian mean velocity, and eddy-induced velocity are level quantities associated with a Cartesian, x, y, z framework. But to estimate the RMI velocity and eddy-induced velocity we first have to calculate the total mean transport in isopycnic coordinates; x, y, σ framework. When calculating the upper-layer RMI transport, σ_1 [Eq. (12)] is the minimum density encountered during the whole time series; σ_2 is that density whose isopycnal surface reaches an annually averaged depth of exactly 20 m, being the thickness of the upper grid box. The depth of this isopycnal, however, varies with time.

The eddy-induced velocity arises from the difference between the RMI velocity and Eulerian mean velocity. However, it is not simply related to an eddy mass flux.

We can decompose $\overline{\mathbf{u}(\sigma)h(\sigma)}$ into a component that is due to the time-averaged flow and a component due to the eddy correlation between layer thickness and velocity variations:

$$\overline{\mathbf{u}(\sigma)h(\sigma)} = \overline{\mathbf{u}}(\sigma)\overline{h}(\sigma) + \overline{\mathbf{u}'(\sigma)h'(\sigma)}, \qquad (15)$$

where primes denote departures from a time average. Now, in general,

$$\int_{\sigma_1}^{\sigma_2} \overline{\mathbf{u}}(\sigma)\overline{h}(\sigma)\, d\sigma \neq \overline{\mathbf{u}}(z)\Delta z; \qquad (16)$$

see the thought experiment below: the Eulerian mean velocity and isopycnal mean velocity (after transformation to z coordinate) are different. As a result, the eddy-induced velocity, or quasi-Stokes velocity, $\mathbf{u}^*$ [see Eq. (14)], and the bolus velocity, $\mathbf{u}^B = \overline{\mathbf{u}'(\sigma)h'(\sigma)}/h$ are also different, while the total mean transport in isopycnic coordinates and the RMI transport in x, y, z coordinates are by definition equal after the first one is transformed to z coordinate.

When the flow is steady, the eddy terms become zero and the Eulerian mean and isopycnal mean velocity are also equal. Therefore, an eddy-induced velocity occurs when there are departures from the time-averaged fields and a bolus velocity occurs when the departures from the mean layer thickness and velocity correlate, but they may differ in magnitude. It seems tentative to associate the departures from a time average and the eddy correlations with mesoscale eddies, but departures of the layer thickness h from its annual average will be seriously affected by the seasonal cycle of the mixed layer when the isopycnal σ_2 is close to the surface.

To illustrate this point further the following thought experiment is suggested: Suppose an eddy-less wind and buoyancy-driven zonal channel. The only meridional flow above a certain sill depth is a constant, wind-driven Ekman flow. The only time variation is that there are two seasons, without any further intraseasonal variations. We consider two layers. Layer 1 has a depth of 40 m in season 1; in season 2 it is completely deflated. Layer 2 has a constant thickness of 20 m. The Ekman transport is always 1 Sv (where 1 Sv $\equiv 10^6$ m^3 s^{-1}). In season 1 this transport is passed to layer 1; in season 2 it is passed to layer 2 (Fig. 2). Let us assume that the column features grid boxes of 20-m thickness. The Ekman flow then always resides in the upper grid box, grid box 1. In this case the Eulerian mean transport is 1 Sv for grid box 1 and 0 Sv for grid box 2.

Now we consider the RMI flow. The RMI transport has to be calculated from the total mean transport in isopycnic coordinates. Both layers 1 and 2 feature an
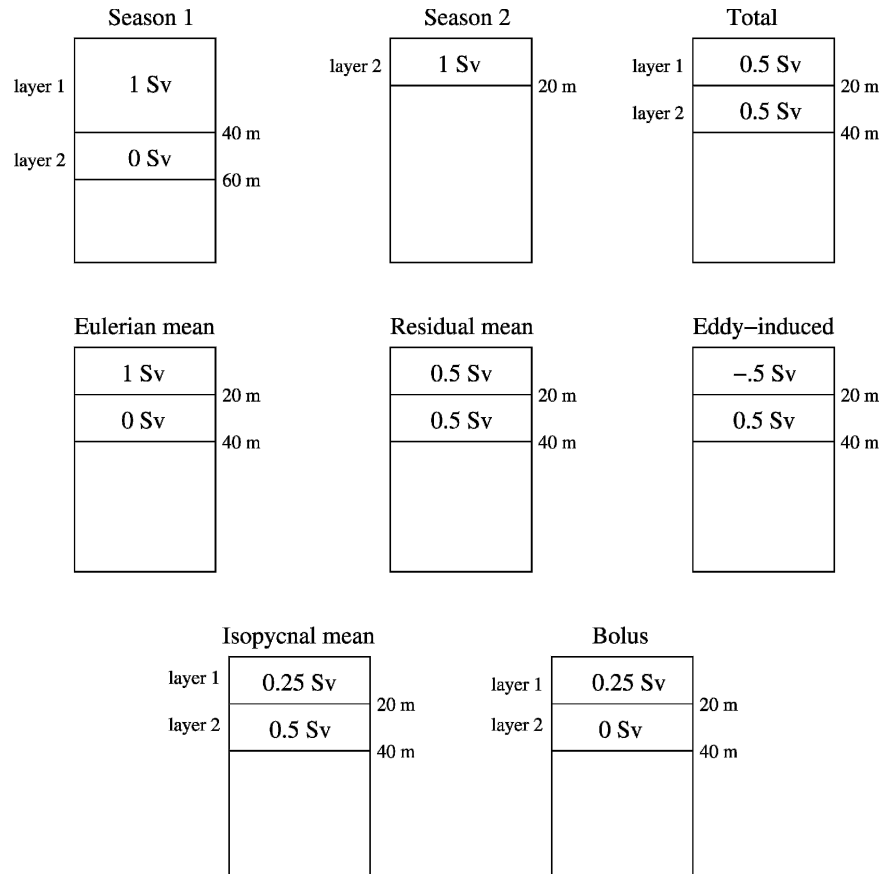
Fig. 2. Schematic diagram of how, in the isopycnal framework, the seasonal cycle induces an eddy-induced transport. Only meridional transports are considered. In this example, the geostrophic transport in the upper layers is always zero, while in the upper layer, Ekman transport always is 1 Sv. In season 1, layer 1 outcrops. In season 2, layer 1 is deflated and layer 2 outcrops. As a result, the Eulerian mean and residual mean isopycnal transports for layers 1 and 2 are different and an eddy-induced transport arises.

Ekman transport of 1 Sv for one-half of the year, so their annually average transport is 0.5 Sv. The annually average thickness of both layers is 20 m, coinciding with the thickness of the upper two grid boxes, which makes the transformation to the RMI transport straightforward. The RMI transport is 0.5 Sv for grid box 1 and 0.5 Sv for grid box 2.

By construction the eddy-induced transport for grid box 1 is –0.5 Sv, while it is 0.5 Sv for grid box 2 (Fig. 2). Because of the seasonal cycle, the RMI flow features an Ekman transport that is redistributed in the vertical, because of a redistribution in density space, while the Eulerian mean flow always assigns the Ekman transport to the upper (Ekman) layer. As a result, the eddy-induced transport in the upper layer opposes the Ekman transport.

The eddy-induced transport cannot be estimated from the bolus transport. We can decompose the total transport in isopycnic coordinates, $\overline{\mathbf{u}h}$, into a transport by the time-mean flow $\overline{\mathbf{u}}\,\overline{h}$ and a bolus transport $\overline{\mathbf{u}'h'}$. The transport by the isopycnally averaged mean flow is 0.25 Sv for layer 1 and 0.5 Sv for layer 2. The bolus transport in layer 1 is 0.25 Sv; in layer 2 it is 0 while h' is 0. Therefore, bolus transport and eddy-induced transport are completely different in this example! Note that in particular for grid box 2 the Eulerian mean flow is zero while the RMI flow is nonzero, although the eddy-correlation term is zero as $h' = 0$. Nevertheless, the eddy-induced transport is nonzero! This illustrates the inequality of Eq. (16).

We can extend this thought experiment by refining the seasons and dividing the year in 365 days. The upper-layer RMI flow will have a fraction p_1 of the Ekman transport, with p_1 as the fraction that the layer was ventilated throughout the year. The upper-layer, eddy-induced transport will equal minus $1 - p_1$ times the

Ekman transport. Below the upper layer, the eddy-induced transport makes up the deficit of $1 - p_1$ times the Ekman transport in the upper-layer RMI flow. The vertical redistribution of the Ekman transport that features the RMI flow does not simply apply to the seasonal, or permanent pycnocline. To understand the depth range of the redistribution we have to remember that the stratification in the residual mean is not defined by the annually averaged density σ in fixed space, but by a density distribution $\hat{\sigma}$ that results from the annually averaged depth of each isopycnal σ (McDougall 1998). In $\hat{\sigma}$ space, the Ekman layer migrates up and down with the seasonal cycle. As a result, the Ekman transport is redistributed in density space over the ventilated residual mean pycnocline, which is the annually averaged depth of the isopycnal bounding the Ekman layer in the coldest day of the year.

In short, in an eddy-less ocean seasonality introduces an eddy-induced transport whose signal tends to increase toward the surface. In particular, in the upper layer such an eddy-induced transport arises from the difference between the Ekman flow and the geostrophic flow below the Ekman layer, and a seasonal cycle that sometimes causes the upper layer to be completely deflated, sometimes to be inflated with water from below the Ekman layer. In $\hat{\sigma}$ space, the Ekman layer moves up and down with the seasonal cycle. This effect is prominent especially in the Southern Ocean. While the upper-layer, annual mean flow consists of the Ekman flow, the RMI flow in the upper layer consists of only a fraction p_1 of the Ekman flow and a fraction $1 - p_1$ of the geostrophic flow below. The resulting eddy-induced transport is just $1 - p_1$ times the difference between the underlying geostrophic flow and the Ekman flow. When the geostrophic flow below the Ekman layer is small, and the fraction p_1 that the upper layer was ventilated is also small, the eddy-induced transport significantly counteracts the Ekman transport.

4. Characteristics of the upper-layer, eddy-induced transport

Figure 3 shows a time series for a point within the ACC (20°E and 60°S) of the depth of the σ level that is on the average 20 m deep, coinciding with the lower bound of the upper grid box. The lower panel shows the associated meridional thickness transport. Indeed, we see that most of the time the layer is deflated and the meridional mass transport is zero. Episodically, the layer is filled with masses of light water and the layer becomes a few hundred meters deep. Although it shares some characteristics with deep convection, what we see is a completely different process. It occurs in

summer. The seasonal heating seems to precondition the water column for the deepening of the surface layer, but both the sudden change in layer depth and the length of the episode that it becomes inflated are associated with a much more nonlinear process than the seasonal cycle itself. The average depth of the upper layers in the annually averaged stratification is determined by a few episodes where these layers reach large depths; the distribution of layer depth is enormously skewed.

Ultimately, it is believed that mesoscale eddies play an essential role in returning the Ekman flow in the Southern Ocean. The associated eddy flux is undoubtedly associated with baroclinic instability. The process described here is not the compensation of the Ekman transport as a whole, but the vertical redistribution of the Ekman transport that characterizes the residual mean isopycnal flow. From redistribution in the vertical arises a compensating eddy-induced mass flux in the surface layer. Transient behavior of a shallow isopycnal is dominated by seasonality and modified by eddies. For a deeper isopycnal, for instance $\sigma_2 = 36.1$, the reverse is the case; it is dominated by mesoscale eddies and modified by seasonality (Fig. 4). In this case, we may assume that baroclinic instability determines the transient behavior of the isopycnal depth and the integrated meridional mass transport. The lower panel of this figure also shows that SSH variability very well reflects the thermocline variability (with shorter timescales superimposed) and that the scaling relations proposed by Holloway (1986) work well if the upper layer is taken deep enough. As a result, we may expect that when the eddy-induced transport is vertically integrated down to the thermocline, the localization that is associated with enhanced baroclinic instability becomes eminent. Figure 5 confirms this. Comparing with Fig. 1 we see a strikingly different picture. The eddy-induced velocity is no longer almost uniformly negative, but shows signs of large rotational fluxes and features maxima that must be associated with spots of increased baroclinic instability. These spots are irregularly spaced in a narrow band associated with the ACC. It is not immediately evident whether the localization of these spots can be explained by topography enhancing the instability of the flow immediately downstream of it, or, that other processes are involved in changing the stability characteristics of the ACC in the downstream direction.

From the fact that the RMI flow features a vertical redistribution of the Ekman transport, an eddy-induced mass transport appears. However, baroclinic instability is also associated with an eddy mass flux that will play a crucial role in compensating the Ekman flow as a

Depth of 20m isopycnal

Meridional eddy-induced transport
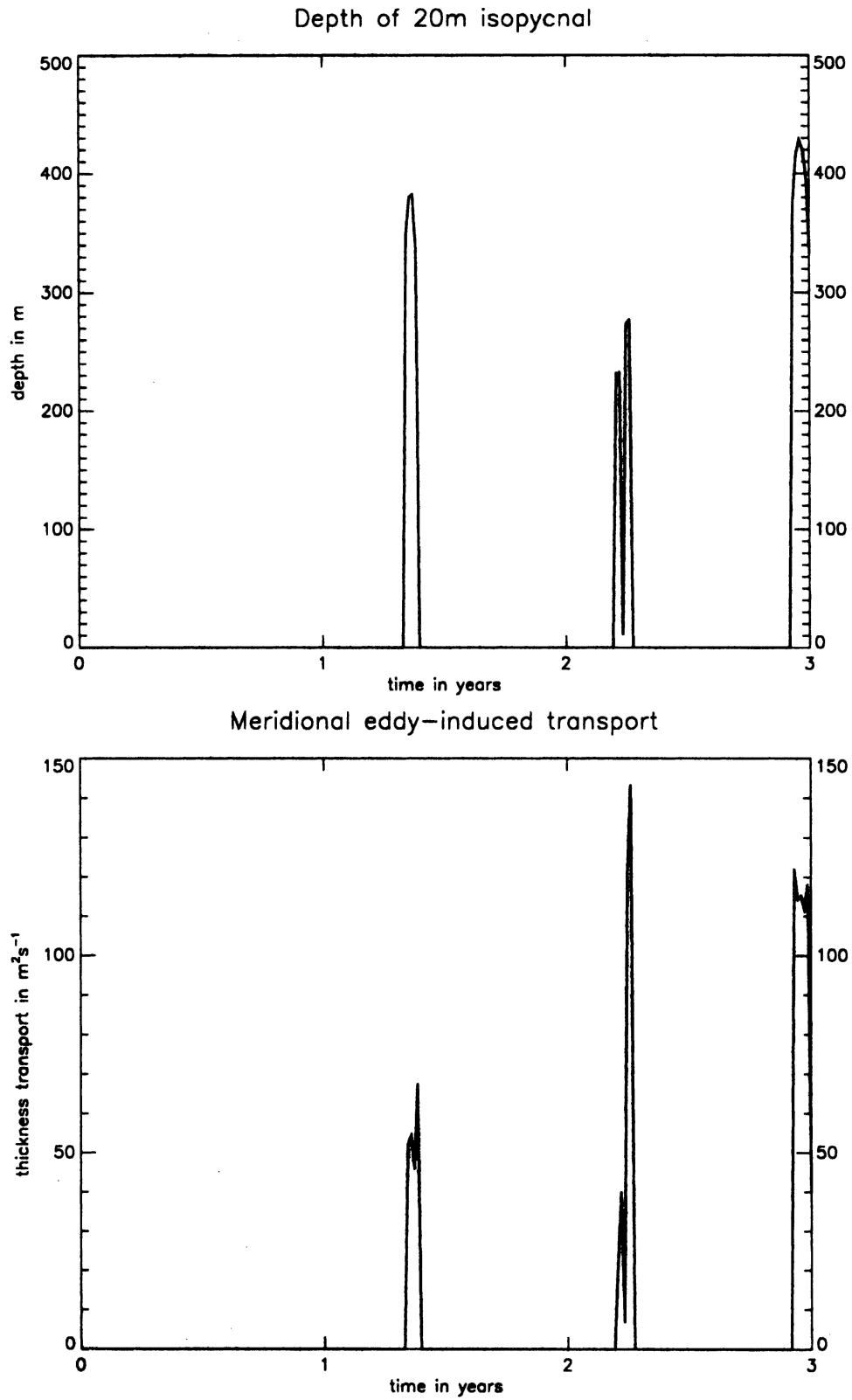
FIG. 3. (top) Three-year time series of the depth of the isopycnal that acquires an average depth of 20 m at 20°E and 60°S, and (bottom) a similar time series for the thickness transport within the isopycnal layer defined by this isopycnal and the sea surface.

Anomalous Thermocline Depth

Sea Surface Height Anomaly
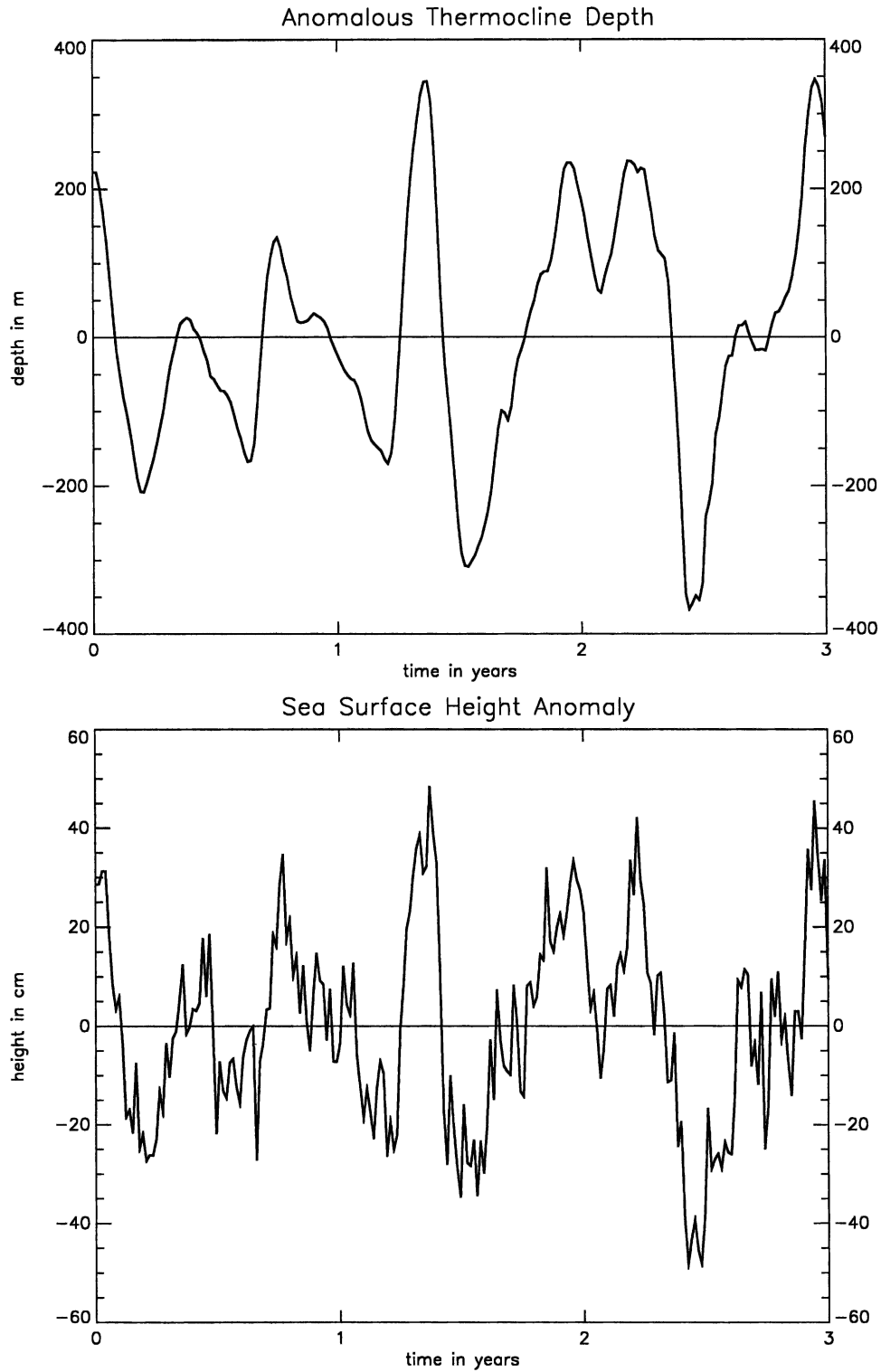
FIG. 4. Similar time series as shown in Fig. 3, but now (top) for the anomalous thermocline depth, defined by the depth of the $\sigma_2 = 36.1$ isopycnal, and (bottom) for the sea surface height anomaly.
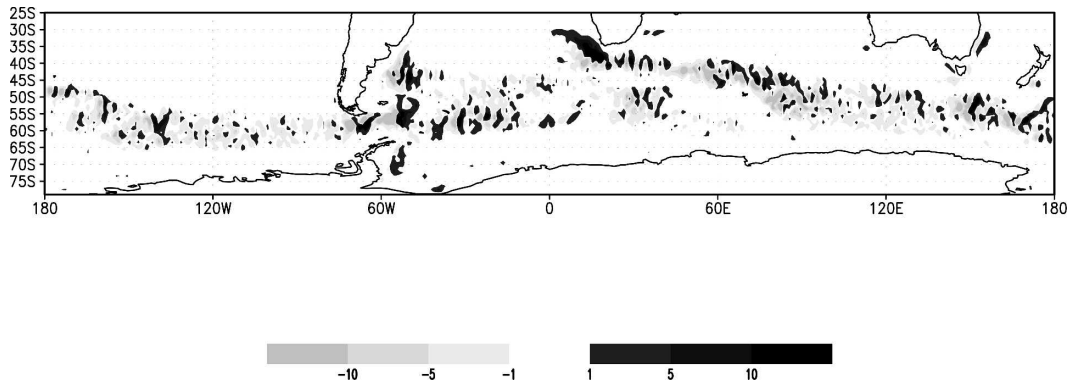
FIG. 5. Same as Fig. 1, but now integrated over the upper 13 layers to a depth of 554.69 m.

whole. Both components of the eddy flux will be largest in the thermocline, but their vertical distribution is dissimilar. The first component peaks in the upper layer where it is poleward; below the Ekman layer it will change sign and become equatorward. We may expect that it is compensated within the upper thermocline. The second component will be poleward in the upper thermocline; change sign at middepth and become equatorward below the sill depth in the channel; the mirror image of the Deacon cell. Figure 6 confirms this picture. It shows the vertical distribution of the eddy fluxes at 48°S, where the zonally integrated Ekman

transport in the Southern Ocean peaks. The eddy fluxes associated with baroclinic instability have been calculated by subtracting the eddy-induced flux that arises from the redistribution of the Ekman transport in the RMI flow from the total eddy-induced mass flux, neglecting other processes. The eddy-induced mass flux associated with baroclinic instability is much too small to compete with the eddy-induced mass flux associated with the Ekman redistribution. In the surface-layer, the eddy-induced mass flux is completely determined by the vertical redistribution of the Ekman transport that features the RMI flow.
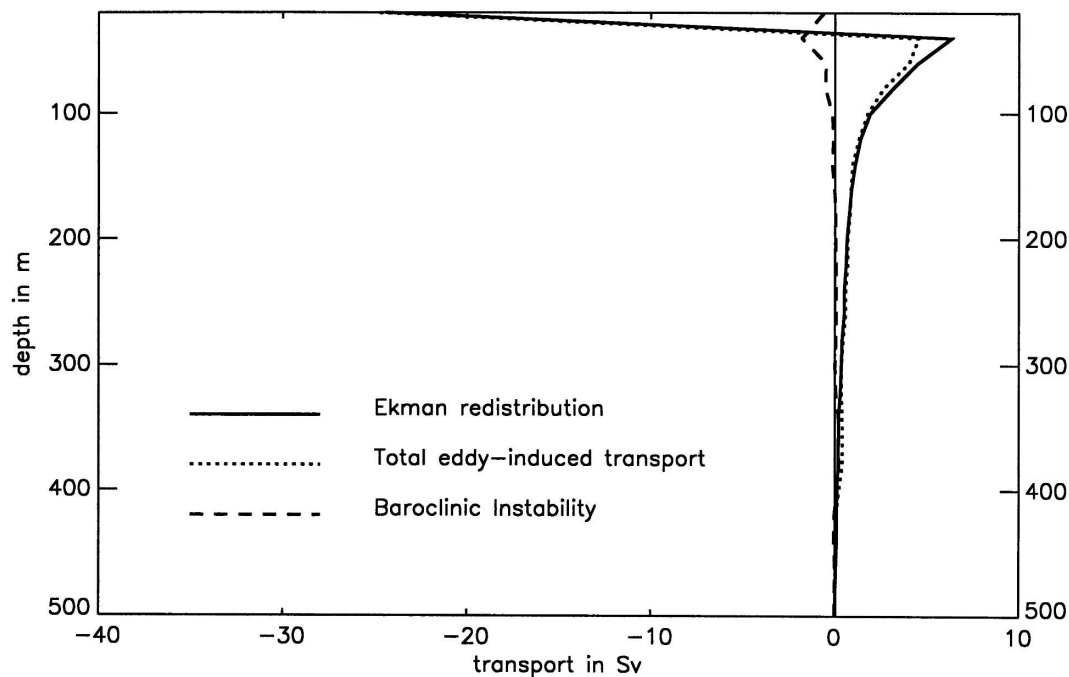
FIG. 6. Vertical distribution of the eddy-induced transport at 48°S, integrated over layers of 20-m thickness, and its decomposition in the vertical redistribution of the Ekman flow and the component associated with baroclinic instability.
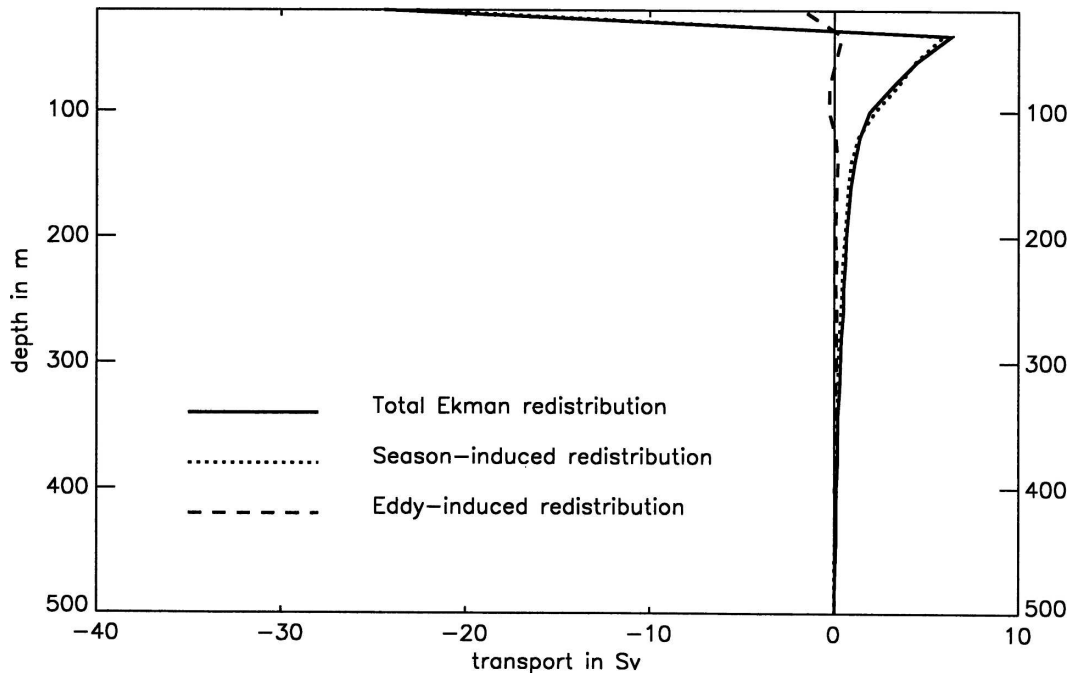
FIG. 7. Same as Fig. 6, but now for the eddy-induced transport associated with the vertical distribution of the Ekman flow decomposed in a seasonal-induced component and a component due to mesoscale eddies.

The very skewed distribution of layer depth of the upper layers that arises from the episodic deepening of these layers, as shown in Fig. 3, suggests that, besides the seasonal cycle, mesoscale eddies might have a strong impact on this vertical redistribution. It could very well be that southward-projecting meanders of the ACC in the summer half year cause the upper layers to be filled with warm water. Because of the eddies, the inflation of the upper layers would then occur more intermittently, and the maximum depth they reach would be enhanced. As a result, the residual mean ventilated pycnocline will reach deeper and the eddy-induced, upper-layer mass flux that counteracts the annual mean Ekman flow becomes larger. To check this scenario, 12 monthly means were constructed from the 219 5-day averages and 219 (3×73) new 5-day averages were calculated by linear interpolation between the monthly means. In this case, the eddy-induced transport due to the redistribution of the Ekman transport in the RMI flow is completely due to the seasonal cycle. The difference in Ekman redistribution between the two datasets is due to mesoscale eddies. From Fig. 7 we see that mesoscale eddies hardly have any impact on the Ekman redistribution. Although the seasonal cycle itself is smooth, its impact on the stratification is such that the inflation and deflation of layers near the surface is highly intermittent, even without eddies being present.

5. The cancellation of the Deacon cell

In the OCCAM model the surface eddy mass flux is primarily a consequence of the intermittent deepening of the mixed layer, which redistributes the Ekman transport over isopycnal layers; baroclinic instability plays a much lesser role. However, this can only come about when the residual mean transport and eddy-induced transport are calculated in an isopycnal framework. When the residual mean theory is worked out in geometric coordinates, a vertical redistribution of the Ekman transport is impossible. This brings us back to the problem of definition of residual mean flow that was discussed in section 2. The residual mean flow in isopycnic coordinates (RMI flow) and in geometric coordinates, differ by order α^3, where α is the perturbation amplitude [Eq. (10)], which becomes $O(1)$ near the surface. In other words, these residual mean flows are completely different in the surface layers!

It is often suggested that the net diapycnal flow can be inferred from the residual circulation crossing zonally averaged contours of potential density, but the implication, that the diapycnal diffusion is zero when the residual circulation follows zonally averaged density contours, is not strictly true. In geometric coordinates, a zonally averaged, purely adiabatic along-isopycnal flow will cross the zonally averaged density contours when they tilt in the zonal direction, and vice versa, a
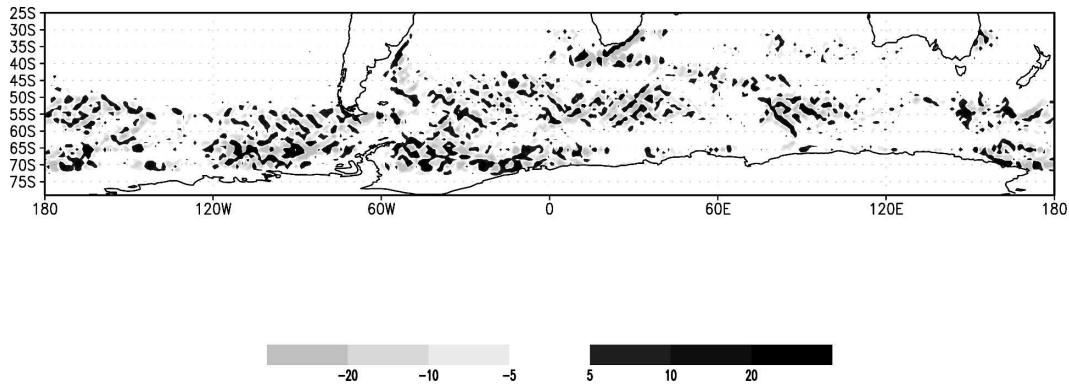
FIG. 8. Same as Fig. 1, but now calculated in a geometric framework according to Eq. (7).

flow that does not cross these contours may have a cross-isopycnal component. For most cases, the differences between the residual mean flow diagnosed in geometric coordinates and the RMI flow will be small, but near the surface differences do matter.

Many authors interpreted the residual circulation as an approximation to the isopycnal (isentropic) mass circulation (Held and Schneider 1999; Eden et al. 2004, manuscript submitted to *J. Phys. Oceanogr.*), but originally the residual circulation was discussed within a framework of geometric coordinates (Andrews and McIntyre 1976) without explicitly referring to the isopycnic mass circulation. Therefore, the residual circulation has a value of its own, especially as the interpretation of isopycnal mass transport in the surface layers where isopycnals outcrop is far from being straightforward.

The difference in the surface layer between the RMI flow and the residual mean flow in geometric coordinates is appreciated by comparing Fig. 1, showing the surface-layer, eddy-induced transport in the isopycnic framework and Fig. 8, showing the surface-layer, eddy-induced transport calculated with Eq. (7), which was advocated by Held and Schneider (1999), Karsten and Marshall (2002), Marshall and Radko (2003). There is no resemblance at all. A uniform poleward eddy transport is absent when it is calculated with Eq. (7). Instead, a localization that is associated with enhanced baroclinic instability is seen, also apparent in the isopycnal eddy mass flux when it is integrated to the base of the pycnocline. When integrated from the sea surface to a depth of 554.69 m, both residual mean theories give almost similar eddy-induced transports. This can be understood as the geometric and isopycnal definitions agree that in the limit that α is small in the interior. As a result, the integral properties between the ocean's surface and the bottom of the seasonal thermocline remain the same, irrespective of the viewpoint. This is due to the fact that the redistribution by Ekman processes cancels out when averaged vertically.

Although Figs. 1 and 8 show completely different patterns for the surface-layer, eddy-induced transport, in both residual mean flow frameworks a similarly small net poleward eddy-induced mass flux results of about 2.5 Sv, an order of magnitude smaller than the Eulerian mean flow. The role of eddies in counteracting the Deacon cell is independent of the coordinate-frame in which the residual mean flow is diagnosed.

In OCCAM the Ekman transport peaks at 48°S with 33 Sv. The Eulerian mean flow features a downwelling of 19 Sv between 48° and 38°S (Fig. 9). The flow returns poleward between 1300- and 2800-m depth, and upwells north of 58°S. This recirculation of 19 Sv is the so-called Deacon cell. When the RMI flow is calculated, there still is a significant Deacon cell albeit slightly weaker; it is now 14 Sv. The difference between Eulerian mean flow and residual mean flow is small in geometric coordinates. The same is true when the meridional overturning is calculated in sigma coordinates (Fig. 10), but now the Deacon cell is much weaker!

This can be explained as follows. The eddy-induced transport reduces the Deacon cell with 5 Sv, independent of the coordinate system in which the residual circulation is calculated. At 48°, S the eddy-induced transport is about 2.5 Sv poleward, but north of 38°S it is 2.5 Sv equatorward, reducing the convergence of the Ekman flow between 48° and 38°S with 5 Sv. A 10-Sv reduction of the Deacon cell is associated with a transformation of the flow from geometric to density coordinates. This effect was first described by Döös and Webb (1994). They showed that in the FRAM model the Deacon cell was canceled when the overturning was calculated in density coordinates. They did not explicitly calculate eddy-induced transports, but averaged isopycnal mass transports in a series of 60 snapshots, which was apparently enough to sample the complete
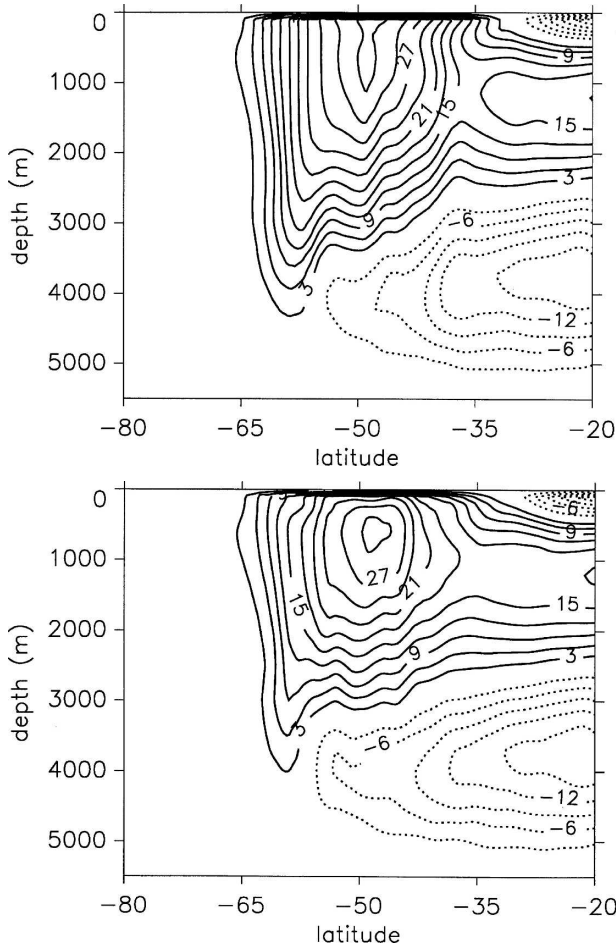
FIG. 9. Zonally integrated streamfunction as a function of latitude and depth for (top) the Eulerian mean velocity and (bottom) the residual-mean isopycnal velocity including eddy transport.

FIG. 10. Zonally integrated streamfunctions as a function of latitude and potential density σ_2 for (top) the annual-mean velocity field and (bottom) residual-mean isopycnal velocity including eddy transport. The density surface $\sigma_2 = 36.8$ used as the upper bound for NADW is also indicated.

eddy field. Döös and Webb (1994) stressed the role of the zonal tilt of isopycnals in the Southern Ocean that makes along-isopycnal recirculations appear as vertical overturning cells in geometric coordinates. These cells combine to form the Deacon cell without any cross-isopycnal flow being involved.

It is tempting to associate these along-isopycnal gyres that are tilted in geometric coordinates as a standing eddy component, which may be eliminated by taking an along- and cross-stream coordinate frame in the horizontal instead of a Cartesian frame (Marshall et al. 1993; Karsten and Marshall 2002). Undoubtedly this will reduce a part of the overturning in geometric coordinates. Most of these gyres, while being connected with the sea surface in some part of the Southern ocean, will cut through, or lie completely within, the depth range that is bounded from below by the base of the winter mixed layer. Although the mixed layer itself is unstratified at any given moment, in an annual average,

the fluid is stratified between the depth of the summer mixed layer (which for simplicity is taken to be equal to the depth of the Ekman layer, h_{Ek}) and the depth of the winter mixed layer h_{ml}. The consequence of the Döös and Webb (1994) mechanism is that $\overline{\Psi}(z = -h_{ml})$ is much smaller than $\overline{\Psi}(z = -h_{Ek}) = -\overline{\tau}/(\rho_0 f)$. To cancel the Deacon cell completely the eddy fluxes below the winter mixed layer have to be associated with a $\Psi^* = -\overline{\Psi}(z = -h_{ml})$. Many two-dimensional models of the residual circulation in the Southern Ocean do not appreciate the Döös and Webb (1994) mechanism and seem to overconstrain the 2D residual mean flow in the Southern Ocean by demanding that the eddy-induced transport below the mixed layer is $\Psi^* = -\overline{\Psi}(z = -h_{Ek})$ (Karsten and Marshall 2002; Olbers and Visbeck 2005).

Figure 10 shows a residual Deacon cell for the RMI

flow of about 4 Sv, which probably may be attributed to drift. The much larger signal of this recirculation in geometric coordinates (Fig. 9) suggests that indeed a purely along-isopycnal circulation on zonally tilting isopycnals gives rise to an apparent diabatically forced overturning cell that crosses zonally averaged contours of density. In OCCAM, cancellation of the Deacon cell is accomplished for 30% by the eddy-induced transport and for 70% by the Döös and Webb mechanism.

6. Discussion

To put the results of this paper in perspective, three topics are further discussed. 1) To what extent are the results affected by a possible too-low eddy energy in the OCCAM model? 2) What is the impact of these results on eddy parameterizations? 3) Can the residual mean circulation overcompensate the Eulerian mean circulation?

a. Impact of too-low eddy energy

To what extent is the result that the eddy-induced surface mass flux is almost completely determined by the vertical redistribution of the Ekman transport in the RMI flow, the consequence of the too-low eddy energy and too-weak baroclinic instability in the eddy-permitting version of OCCAM with its horizontal resolution of 0.25°?

The OCCAM model has been spun up for 12 yr and is still drifting. The spinup time is short enough to assume that the residual circulation is still loosely constraint by the model physics and still heavily constrained by both the Levitus' hydrography, which serves as initial state, and by the bottom topography. If in reality the eddy fluxes would be strong enough to partly cancel the MOC in the Southern Ocean and to reduce the upwelling of NADW there, we would expect to see signs of such behavior in the model. However, we do not see such signs. The only aspect of the circulation in the Southern Ocean that is seriously affected by the eddy fluxes is the recirculation in the MOC that is associated with the Deacon cell (Fig. 10). It is weakened by the eddy fluxes, but complete cancellation is not accomplished, probably because of model drift. As compared with 30°S, there is still some 4–5 Sv extra recirculation at 48°S. It seems safe to take 6 Sv as the upper bound of the amount the eddy flux associated with baroclinic instability could rise. This implies that the eddy flux associated with baroclinic instability could rise from the 4 Sv we find in the present model to 10 Sv in a more realistic, higher-resolution model. This 6 Sv of extra eddy mass flux would have to be divided over

the depth of the residual Deacon cell in $\hat{\sigma}$ space, which is about 700 m—see Lee and Coward (2003). This would not seriously affect the proportion of the two components of the upper-layer, eddy-induced mass transport—namely, one component associated with the vertical redistribution of the Ekman transport in the RMI flow that completely outnumbers another component associated with the baroclinic instability of the flow.

b. The relation with eddy-diffusivity closures

Because in the RMI framework, the upper-layer, eddy-induced mass transport is mainly determined by the vertical redistribution of the Ekman transport, estimating the surface eddy flux with a downgradient eddy-diffusivity closure does not work well. Fitting an exponential profile to Fig. 6 it is found that the vertical (re)distribution of the Ekman flow in the RMI flow can be approximated by

$$E(z) = \frac{E_{\text{tot}}}{H} \exp(-z/H), \qquad (17)$$

where E_{tot} is the total Ekman transport across a line segment δx and $E(z)$ is the vertical distribution of the Ekman flow (Sv m^{-1}). In the Southern Ocean a good value for H is $H = 60$ m. This distribution yields a zonally integrated transport of 9.6 Sv by the RMI flow across 48°S for the upper 20 m, being 28% of the total Ekman transport. The eddy-induced mass flux is -24.4 Sv, being -72% of the Ekman transport. In principle, in Eq. (17) H is a function of x and y. It may be estimated from the data by noting that aH is the depth of the annually averaged isopycnal σ_{aH} for which it holds that throughout the year a fraction of $\exp(-a)$ of the surface values of σ_0 will be denser than σ_{aH}; a fraction of $1 - \exp(a)$ will be less dense, where a is an arbitrary number.

The remaining eddy flux that is associated with baroclinic instability may be associated with a downgradient eddy diffusivity, but the appropriate value for K is about an order of magnitude less (100–200 m^2 s^{-1}) than the values chosen by, for example, Karsten and Marshall (2002) and Speer et al. (2000) when they related the total eddy-induced mass flux to an eddy diffusivity closure within a residual mean framework in geometric coordinates. If we assume that OCCAM underestimates the eddy flux associated with baroclinic instability with 6 Sv at maximum, the upper bound for K in the surface layers would become 250–500 m^2 s^{-1}.

Values for K of a few 100 m^2 s^{-1} compare well with the fit made by Olbers and Ivchenko (2001) in the Southern Ocean for the POP model, below a depth of 500 m. For the upper levels, however, these values seem

low relative to the results that Bryan et al. (1999) obtained for the same model. Although both Bryan et al. (1999) and Olbers and Ivchenko (2001) estimated eddy diffusivities with a different method than used here, these results strongly suggest that baroclinic instability is more prominent in the higher-resolution POP model than in OCCAM and that the role of the eddy transport in the cancellation of the Deacon cell in the POP model would be larger. When this indeed should be the case, it would be pertinent to analyze whether the Döös and Webb (1994) mechanism is less prominent in the POP model than in both OCCAM and FRAM, or, whether it would become less prominent with higher resolution.

c. Can the eddy-induced transport overcompensate the Ekman transport?

Values for K of 250–500 m^2 s^{-1} are far too low to yield a residual mean circulation that opposes the Eulerian mean circulation in the upper layers at the equatorward flank of the ACC, as obtained by, for example, Karsten and Marshall (2002). In Karsten and Marshall's model, this poleward flow does not counteract the MOC, as it subducts near the Antarctic convergence and returns equatorward within the thermocline. Such a circulation, however, implies a thermally indirect Ferrel cell across the polar front that is so strong that it overcomes the Eulerian mean flow. In general, the eddy-driven Ferrel cell opposes the wind scale, Eulerian mean overturning across midlatitude jets (Bryan 1991; Drijfhout 1994) by smoothing the isopycnal slopes that are set by the wind forcing. But in eddy-resolving models the net residual mean overturning always opposes the Ferrel cell, as the latter is weaker than the wind-scale Eulerian mean overturning cell. As the cross-frontal scale of the buoyancy forcing is larger than the cross-frontal scale of the surface density field, net (wind driven) downwelling at the equatorward side, and upwelling at the polar side is necessary to maintain the surface signature of the front. If the Ferrel cell would be so strong that the residual mean circulation changes direction, it would destroy its own source of available potential energy. It should be noted, however, that the idealized model of Marshall (1997) does allow for a residual mean flow opposing the Eulerian mean flow at the surface in the Southern Ocean, while maintaining thermodynamic equilibrium. The meridional density distribution at the surface, however, is very smooth in Marshall's (1997) model and does not allow for frontal structures. Therefore, such a circulation does not seem realistic because it would not be able to maintain the surface signature of the polar front in the Southern Ocean.

7. Summary and conclusions

The surface-layer, eddy-induced mass flux was analyzed in the OCCAM eddy-permitting ocean model to investigate the cause of the apparent paradox that the surface-layer, eddy-induced transport in the Southern Ocean is almost uniformly poleward in the model, scaling with the local Ekman transport, while other models and observations suggest an enhancement of eddy fluxes downstream of topography with large rotational components. Although the baroclinic instability that should give rise to the eddy fluxes is significantly underestimated in the OCCAM model, integrated over the thermocline depth the eddy fluxes do show topographic localization. Moreover, thermocline depth variability associated with baroclinic instability is well reflected by the SSH variability, especially when the shorter time scales of SSH variability are filtered.

The eddy fluxes associated with baroclinic instability, however, make up only a small portion of the total eddy mass flux in the surface layer. The RMI flow features a vertical redistribution of the Ekman transport over the stack of layers that eventually become ventilated during the seasonal cycle. As a result, the upper-layer, RMI mass transport consists of only a fraction of the Ekman transport. The eddy-induced transport, being the difference between the two, is mainly determined by the nonattendance of the Ekman transport in the upper-layer RMI flow. In $\hat{\sigma}$ space, the Ekman layer moves up and down with the seasonal cycle. A time series of the upper-layer thickness (of, say, 20-m depth in the annual average) accordingly shows this layer to be deflated for most of the time; while occasionally it reaches depths of a few hundred meters. Although the driving is opposite (heating instead of cooling), the episodic deepening of the layer mimics the intermittency of convective mixing events. Both are basically driving by the seasonal cycle in buoyancy forcing, but their intermittency results from the nonlinearity that is associated with the deepening of isopycnals.

The vertical redistribution of the Ekman transport in the RMI flow may be approximated by an exponential profile with an e-folding layer depth of 60 m. When integrated over the upper 20 m, at 48°S this yields an RMI transport of 28% of the Ekman transport, and an eddy-induced mass transport of −72% of the Ekman transport. The remaining eddy transport associated with baroclinic instability is at least an order of magnitude less in the upper layer. It is associated with eddy diffusivities of only a few hundred meters per second. Although the eddy fluxes associated with baroclinic instability are underestimated in the OCCAM model, it is argued that these fluxes are too small to cause the total,

upper-layer eddy-induced mass flux to overcome the Eulerian mean flow, resulting in a residual mean flow that opposes the Eulerian mean flow.

The eddy-induced transport that opposes the wind-driven Ekman flow only partially compensates the Deacon cell. The associated overturning cell is about 5 Sv, responsible for a cancellation of the Deacon cell of about 30%. In geometric coordinates, a strong signature (14 Sv) of the Deacon cell remains for the residual mean flow. Only after transformation to density coordinates a further reduction with 10 Sv is obtained. In accordance with Döös and Webb (1994) the zonal tilt of isopycnals makes along-isopycnal recirculations appear as vertical overturning cells in geometric coordinates. These cells combine to form the Deacon cell without any cross-isopycnal flow being involved. They disappear in the isopycnal framework. There is no eddy-induced transport involved in their cancellation.

REFERENCES

Andrews, D. G., and M. E. McIntyre, 1976: Planetary waves in horizontal and vertical shear: The generalized Eliassen–Palm relations and the mean zonal acceleration. *J. Atmos. Sci.,* **33,** 2031–2048.

——, J. Holton, and C. Leovy, 1987: *Middle Atmospheric Dynamics.* Academic Press, 489 pp.

Best, S. E., V. O. Ivchenko, K. J. Richards, R. D. Smith, and R. C. Malone, 1999: Eddies in numerical models of the Antarctic Circumpolar Current and their influence on the mean flow. *J. Phys. Oceanogr.,* **29,** 328–350.

Bryan, K., 1991: Poleward heat transport in the ocean. *Tellus,* **43,** 104–115.

——, J. K. Dukowicz, and R. D. Smith, 1999: On the mixing coefficient in the parameterization of bolus velocity. *J. Phys. Oceanogr.,* **29,** 2442–2456.

Bryden, H. L., and R. A. Heath, 1985: Energetic eddies at the northern edge of the Antarctic Circumpolar Current. *Progress in Oceanography*, Vol. 14, Pergamon, 65–87.

Döös, K., and D. J. Webb, 1994: The Deacon cell and other meridional cells of the Southern Ocean. *J. Phys. Oceanogr.,* **24,** 429–442.

Drijfhout, S. S., 1994: On the heat transport by mesoscale eddies in an ocean circulation model. *J. Phys. Oceanogr.,* **24,** 353–369.

——, P. de Vries, K. Döös, and A. C. Coward, 2003: Impact of eddy-induced transport on the Lagrangian structure of the upper branch of the thermohaline circulation. *J. Phys. Oceanogr.,* **33,** 2141–2155.

Gent, P. R., and J. C. McWilliams, 1990: Isopycnic mixing in ocean circulation models. *J. Phys. Oceanogr.,* **20,** 150–155.

Gille, S., 1997: The Southern Ocean momentum balance: Evidence for topographic effects from numerical model output and altimeter data. *J. Phys. Oceanogr.,* **27,** 2219–2231.

——, 2003: Float observations of the Southern Ocean. Part II: Eddy fluxes. *J. Phys. Oceanogr.,* **33,** 1182–1196.

Hallberg, R. W., and A. Gnanadesikan, 2001: An exploration of the role of transient eddies in determining the transport of a zonally reentrant current. *J. Phys. Oceanogr.,* **31,** 3312–3330.

Held, I. M., and T. Schneider, 1999: The surface branch of the zonally averaged mass transport circulation in the troposphere. *J. Atmos. Sci.,* **56,** 1688–1697.

Holloway, G., 1986: Estimation of oceanic eddy transports from satellite altimetry. *Nature,* **323,** 243–244.

Johnson, G. C., and H. L. Bryden, 1989: On the size of the Antarctic Circumpolar Current. *Deep-Sea Res.,* **36,** 39–53.

Karsten, R. H., and J. Marshall, 2002: Constructing the residual circulation of the ACC from observations. *J. Phys. Oceanogr.,* **32,** 3315–3327.

——, H. Jones, and J. Marshall, 2002: The role of eddy transfer in setting the stratification and transport of a circumpolar current. *J. Phys. Oceanogr.,* **32,** 39–54.

Lee, M.-M., and A. Coward, 2003: Eddy mass transport for the Southern Ocean in an eddy-permitting global ocean model. *Ocean Modell.,* **5,** 249–266.

MacCready, P., and P. B. Rhines, 2001: Meridional transport across a zonal channel: Topographic localization. *J. Phys. Oceanogr.,* **31,** 1427–1439.

Marshall, D., 1997: Subduction of water masses in an eddying ocean. *J. Mar. Res.,* **55,** 201–222.

Marshall, J., and T. Radko, 2003: Residual-mean solutions for the Antarctic Circumpolar Current and its associated overturning circulation. *J. Phys. Oceanogr.,* **33,** 2341–2354.

——, D. Olbers, H. Ross, and D. Wolf-Gladrow, 1993: Potential vorticity constraints on the dynamics and hydrography of the Southern Ocean. *J. Phys. Oceanogr.,* **23,** 465–487.

McDougall, T. J., 1998: Three-dimensional residual mean theory. *Ocean Modeling and Parameterization,* E. P. Chassignet and J. Veron, Eds., Kluwer, 269–302.

McIntosh, P. C., and T. J. McDougall, 1996: Isopycnal averaging and the residual mean circulation. *J. Phys. Oceanogr.,* **26,** 1655–1660.

Olbers, D., and V. O. Ivchenko, 2001: On the meridional circulation and balance of momentum in the Southern Ocean of POP. *Ocean Dyn.,* **52,** 79–93.

——, and M. Visbeck, 2005: A model of the zonally averaged stratification and overturning in the Southern Ocean. *J. Phys. Oceanogr.,* **35,** 1190–1205.

Phillips, H. E., and S. R. Rintoul, 2000: Eddy variability and energetics from direct current measurements in the Antarctic Circumpolar Current south of Australia. *J. Phys. Oceanogr.,* **30,** 3050–3076.

Speer, K., S. R. Rintoul, and B. M. Sloyan, 2000: The diabatic Deacon cell. *J. Phys. Oceanogr.,* **30,** 3212–3222.

Stammer, D., 1997: Global characteristics of ocean variability estimated from regional TOPEX/Poseidon altimeter measurements. *J. Phys. Oceanogr.,* **27,** 1743–1769.

Visbeck, M., J. Marshall, T. Haine, and M. Spall, 1997: Specification of eddy transfer coefficients in coarse-resolution ocean circulation models. *J. Phys. Oceanogr.,* **27,** 381–402.

Webb, D. J., A. C. Coward, B. A. de Cuevas, and C. S. Gwilliam, 1997: A multiprocessor ocean general circulation model using message passing. *J. Atmos. Oceanic Technol.,* **14,** 175–183.